DETECTING DEBONDED REGIONS THROUGH THE FACE SHEETS OF SANDWICH STRUCTURES USING MIRROR ASSISTED IMAGING TECHNIQUES

H. L. Emily Leung*, Janice M. Dulieu-Barton, and Ole T. Thomsen

*emily.leung@bristol.ac.uk

Bristol Composites Institute, School of Civil, Aerospace, and Mechanical Engineering, University of Bristol, UK

Engineering and Physical Sciences Research Council

CERTIFICATION FOR DESIGN: RESHAPING THE TESTING PYRAMID

University of BRISTOL

UNIVERSITY OF BATH

University of Southampton

UNIVERSITY OF EXETER

Introduction

Sandwich structures

- High bending stiffness and strength to weight ratio

Face/core debonding occurs during:

- Manufacture, and
- In-service

Previous studies have shown that the combined use of FE analysis and full-field imaging techniques can

- Identify the crack tip response at the face sheet/core interface, and
- Subsequent damage progression

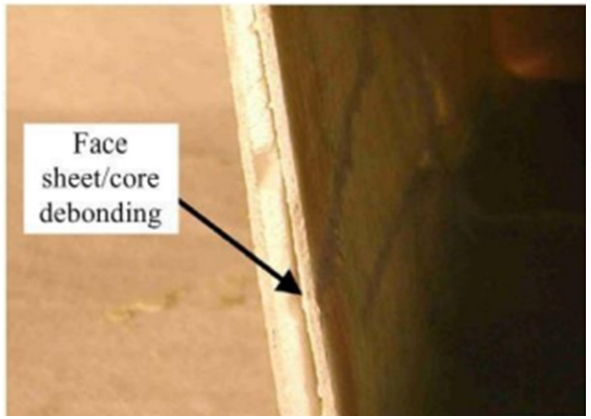

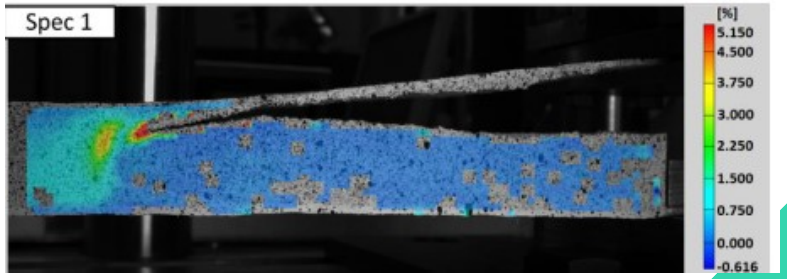

Engineering and Physical Sciences Research Council

CERTIFICATION FOR DESIGN: RESHAPING THE TESTING PYRAMID

University of BRISTOL

Diab

Limitation

Complex and curved geometries

No optical access to damaged region

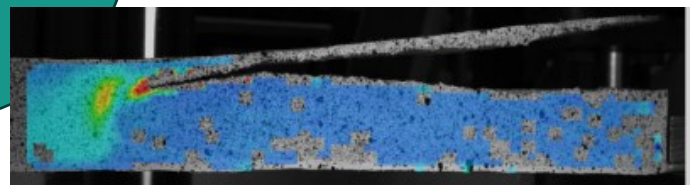

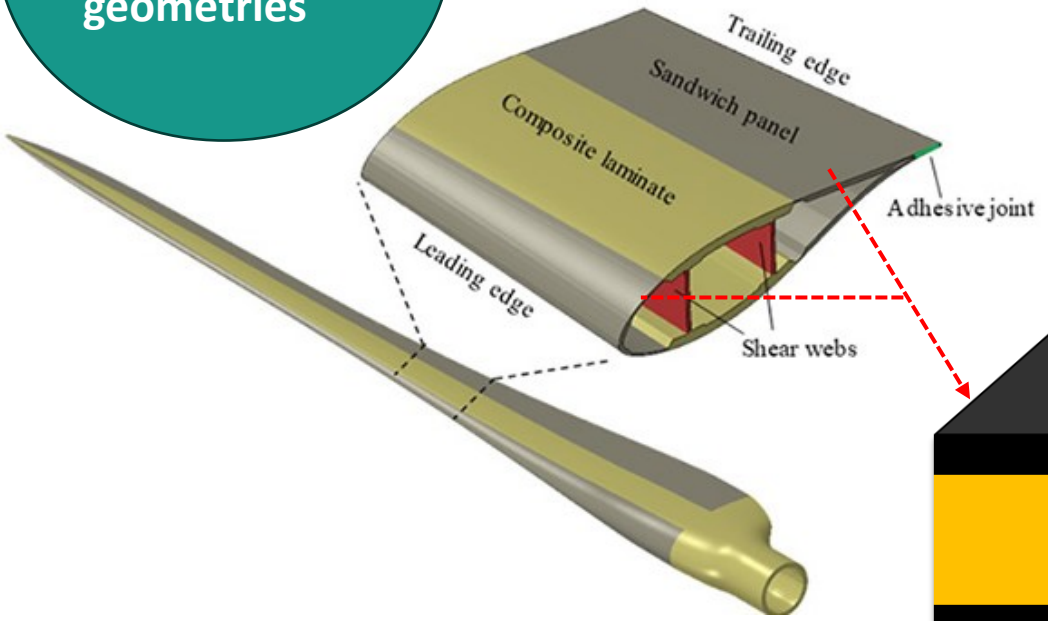

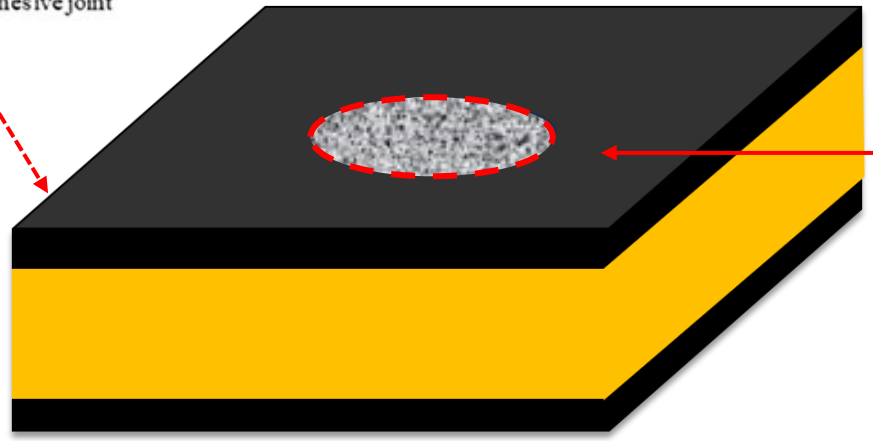

Debond at the facesheet/core interface

Engineering and Physical Sciences Research Council

CERTIFICATION FOR DESIGN: RESHAPING THE TESTING PYRAMID

University of BRISTOL

Diab

Aim & Objectives

To identify facesheet/core interface debond/delamination through the thin face sheets of sandwich structures by:

- Combining the full field imaging techniques of Digital Image Correlation (DIC) and Thermoelastic Stress Analysis (TSA) to detect and characterize debond growth
- Using a mirror-assisted imaging methodology developed as part of the PhD project to view inaccessible regions and extend the field of view of cameras

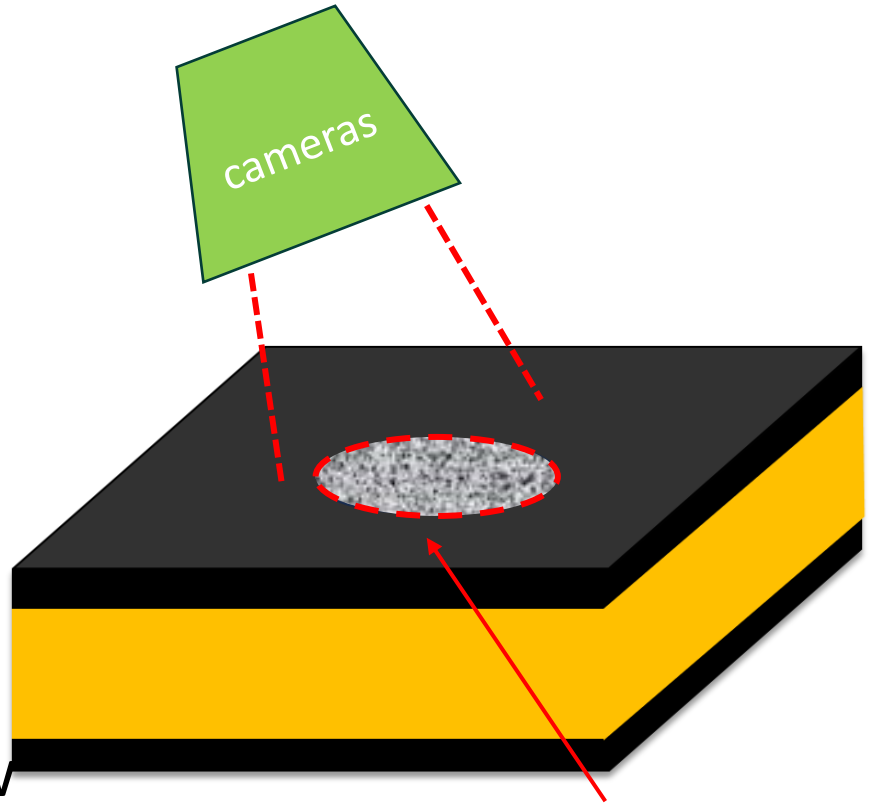

Debond at the facesheet/core interface

Thermoelastic stress analysis (TSA)

- TSA utilizes an IR camera to obtain a series of images from a component under a cyclic load
- The thermoelastic response, ΔT, is obtained from the image series
- ΔT is related to the stresses by $\frac{\Delta T}{T_0} = \frac{(\alpha_1 \Delta\sigma_1 + \alpha_2 \Delta\sigma_2)}{\rho C_p}$

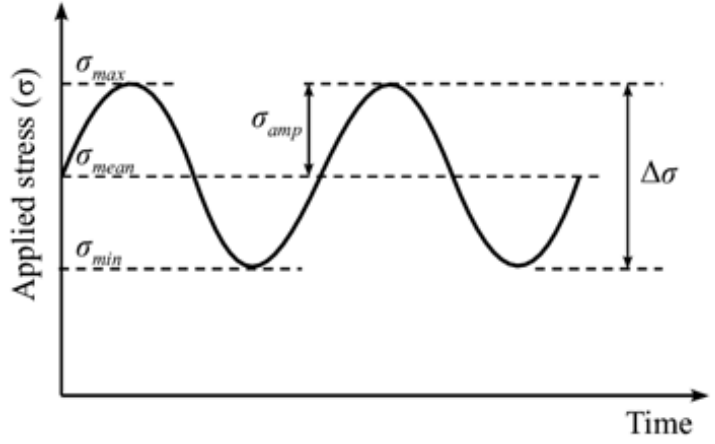

α is the coefficient of thermal expansion

T_0 is the surface temperature

ρ is the density

C_p is the specific heat at constant pressure

$\Delta\sigma$ is the change in stress

- Assumption is no heat transfer takes place
- Carbon fibre is highly conductive, so heat transfer occurs at low loading frequency
- Explore using non-adiabatic response to 'see' through the face sheet

Combining TSA and DIC

- White speckle patterns on a black background are applied on the surface of the face sheet
- DIC tracks the movement of the speckles and provides the deformations
- ε_x, ε_x and ε_{xy} is obtained from the surface deformations
- Converted to the stress components using E_1, E_2, G_{12}, v_{xy} (known elastic constants)
- $\frac{\Delta T}{T_0}$ can be derived by knowing α, ρ , C_p and the surface emissivity
- Calculated $\frac{\Delta T}{T_0}$ is independent of heat transfer

Specimen and loading configuration

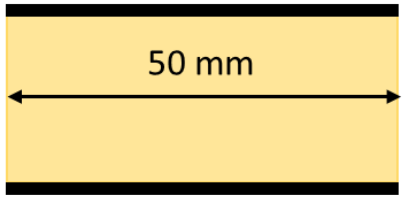

Cross sectional view

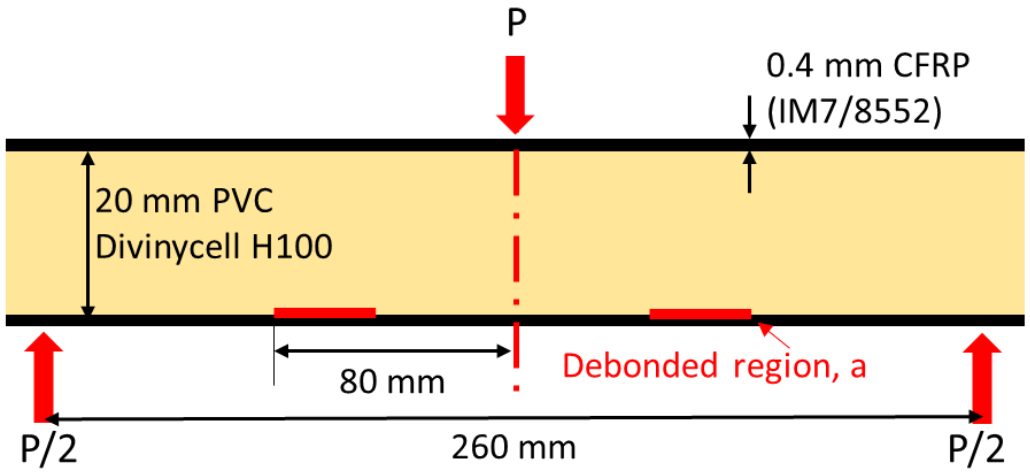

Front view

Specimen configuration

Face sheet lay-up: (0)3

Core density : 100 kg/m^3

Debonded region, a: 10 mm, 20 mm, 30 mm

Loading details for TSA

Loading (N)		a (mm)		
Mean	Amplitude	10	20	30
-400	± 300	√	√	√
-450	± 350	√	√	√
-500	± 400	√	√	√
-550	± 450	√	√	X

Loading Frequency (Hz)						
1.1	2.1	3.1	4.1	6.1	10.1	12.1
√ (with DIC)	√	√	√	√	√	√

Experimental set-up

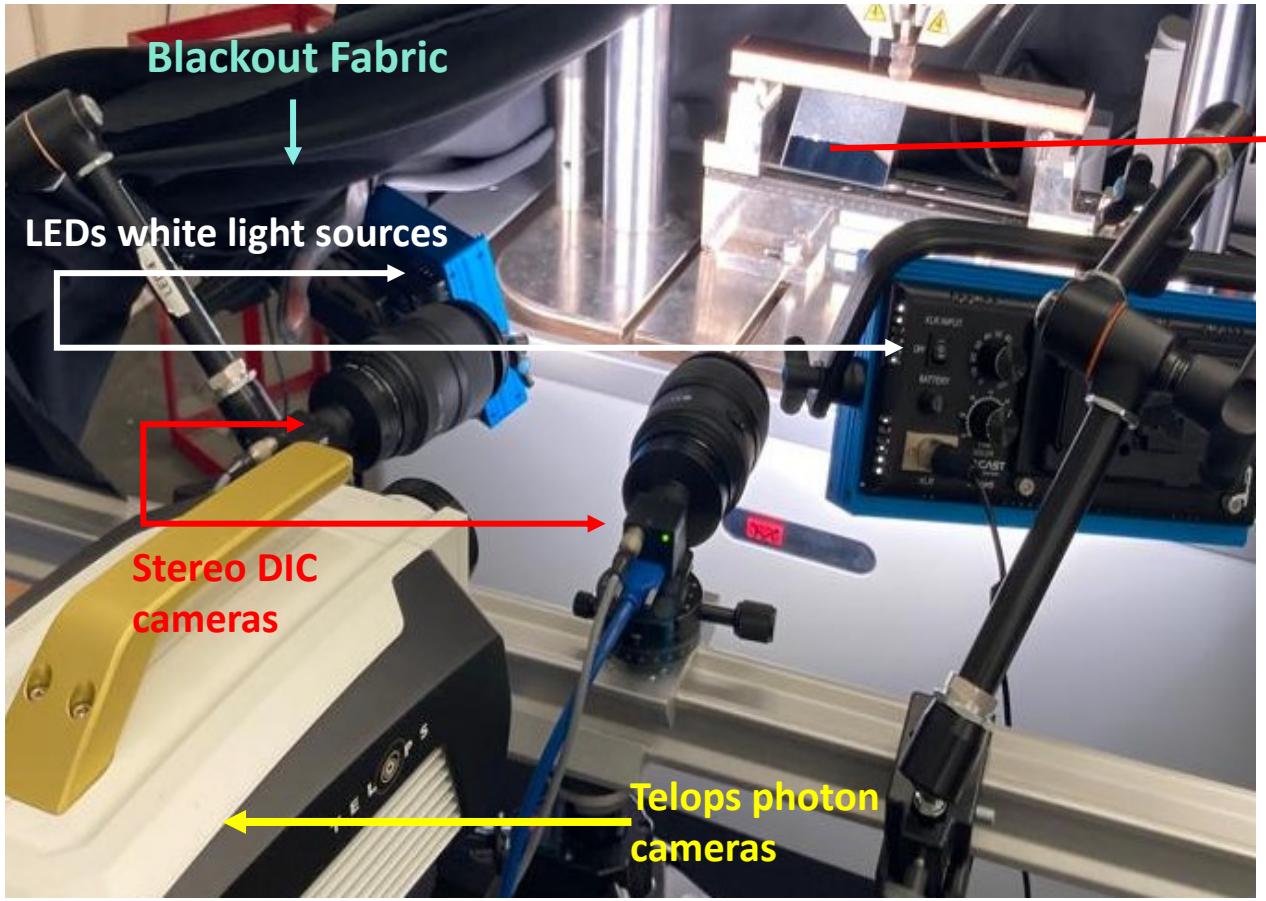

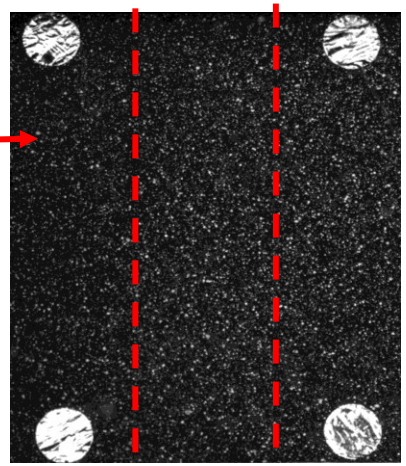

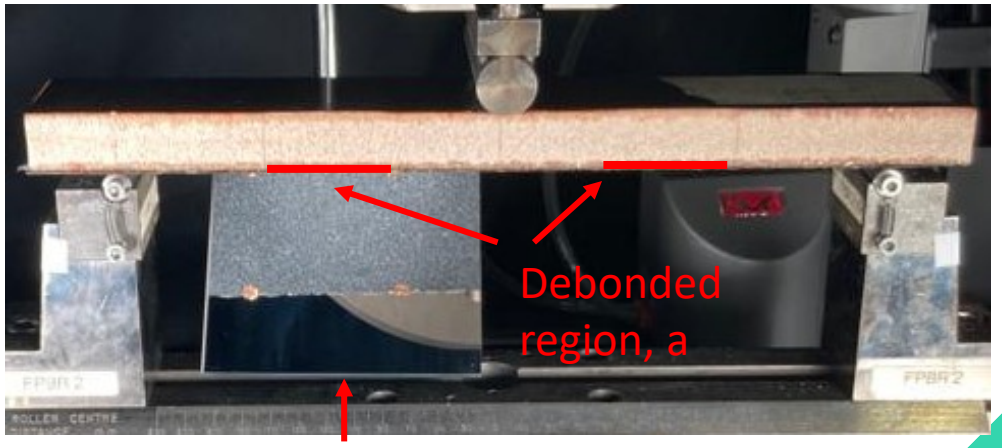

Front coated mirror at 45°

Effect of frequency on ΔT

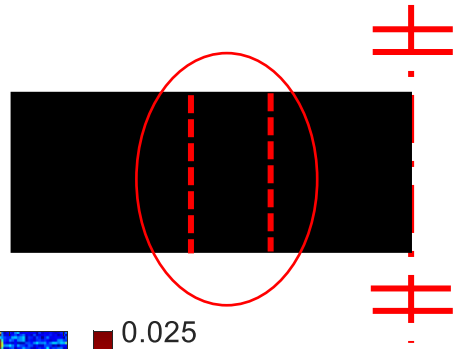

10mm debonded specimen loaded at -550 N with ±450N amplitude

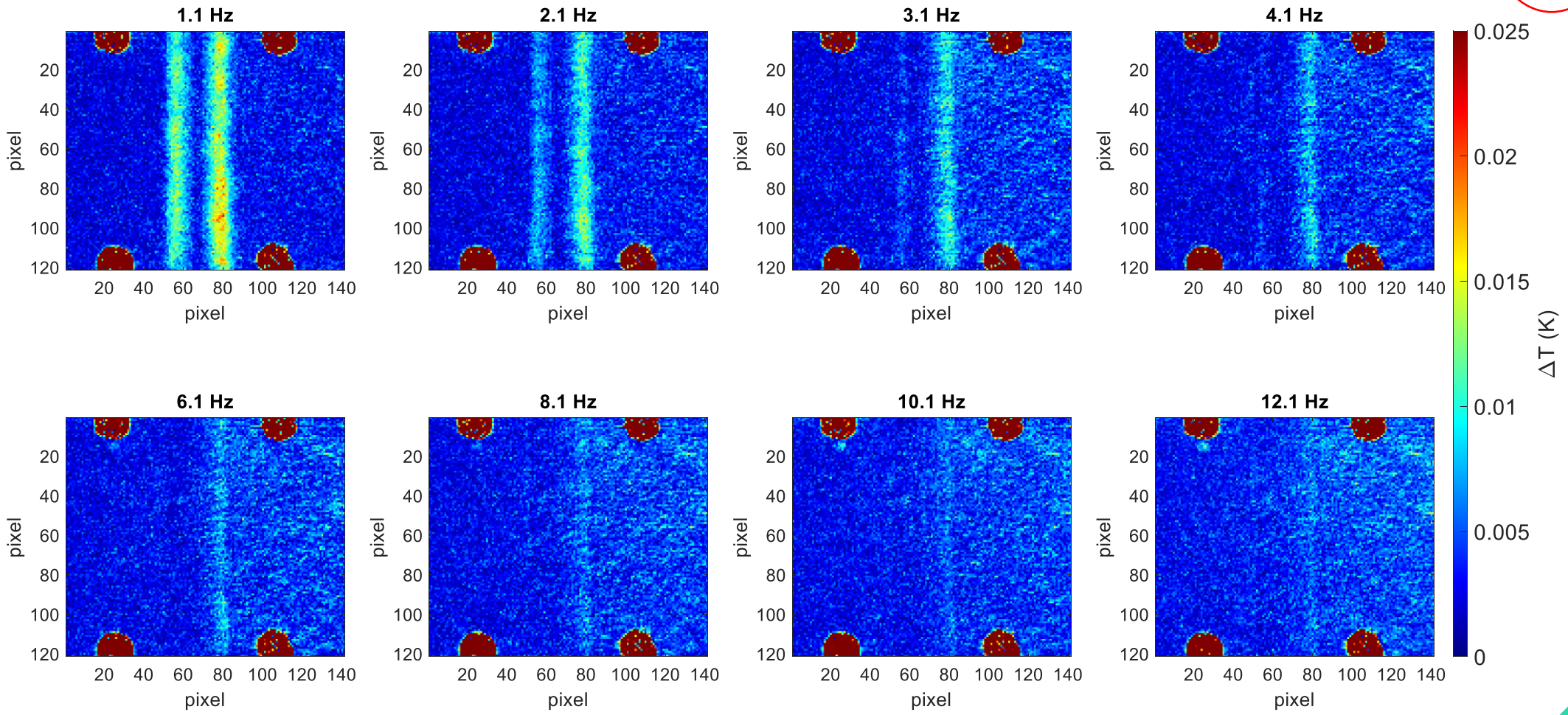

Engineering and Physical Sciences Research Council

CERTIFICATION FOR DESIGN: RESHAPING THE TESTING PYRAMID

University of BRISTOL

Diab

Effect of debond size on ΔT

Average ΔT taken along green line

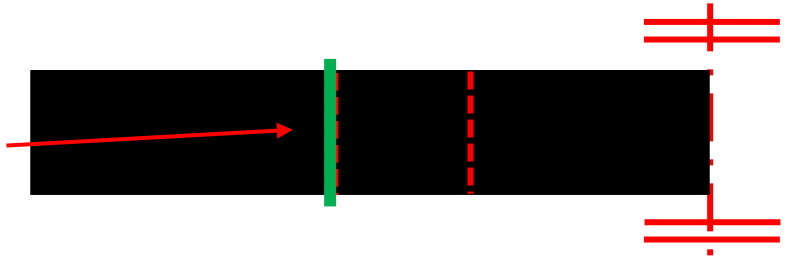

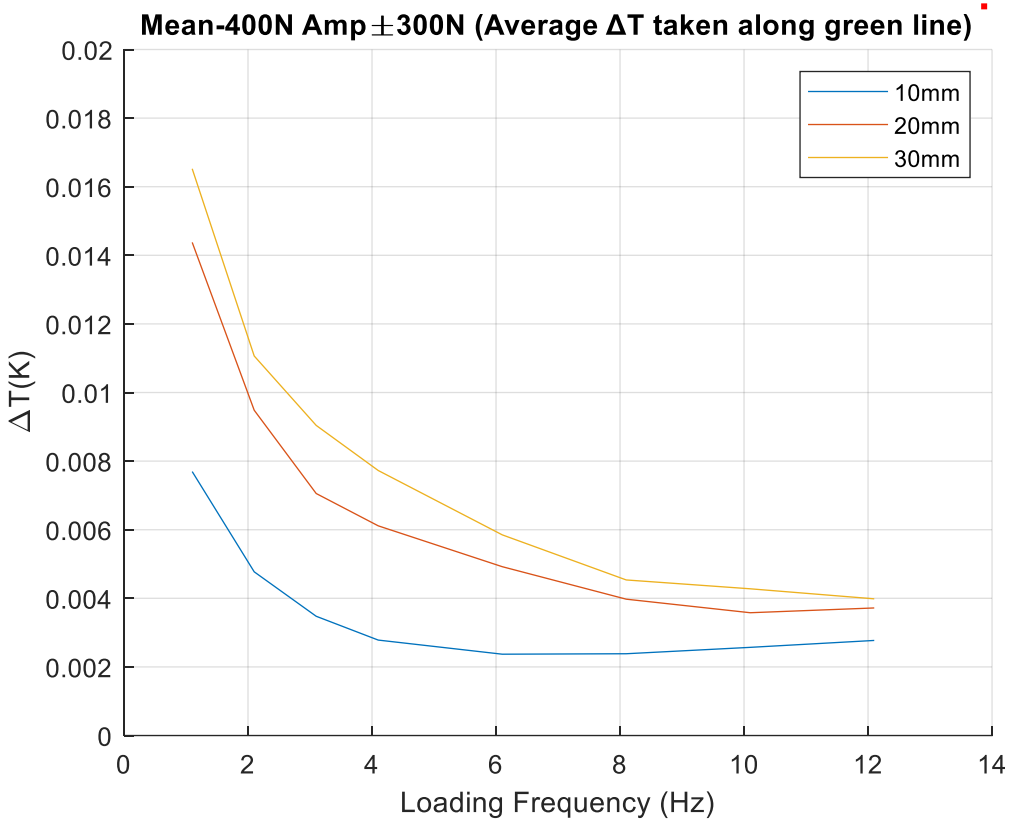

Trends are similar regardless of debond size:

- High thermoelastic response at low frequencies
- Decreases exponentially with increased loading frequency
- Plateau at approx. 5 Hz

Specimens with larger debonds

- Higher thermoelastic response
- Unable to transfer longitudinal stress at the tips/edges of the debond
- ΔT at 30 mm >20mm > 10mm

Effect of loading amplitude

Average ΔT taken along green line

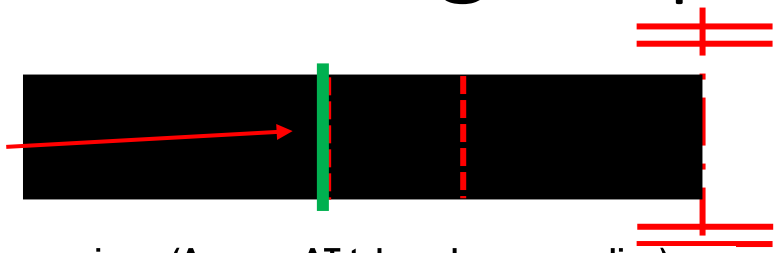

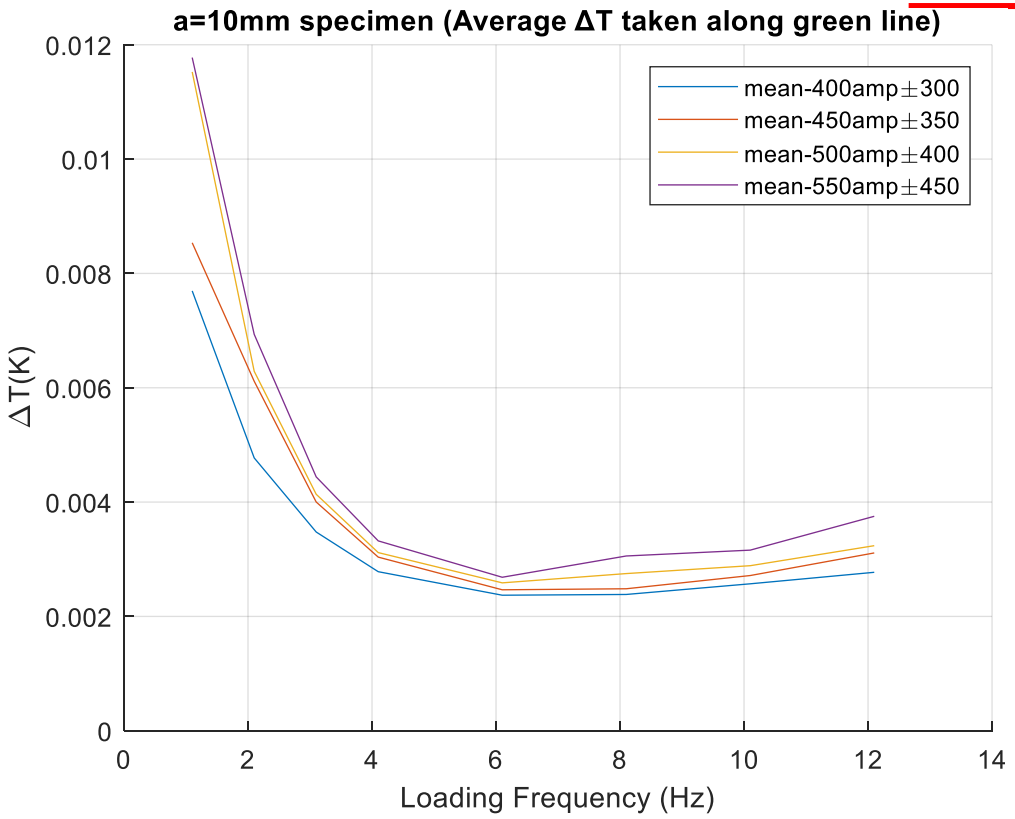

Specimens loaded at higher amplitude give higher thermoelastic responses

Trends are similar regardless of loading amplitude:

- High thermoelastic response at the start
- Decreases with increased loading frequencies
- Plateau at approx. 5 Hz
- Increase in thermoelastic response after 6 Hz

To observe the damaged region at the interface through the face-sheets, heat conduction from the sub-surface at low loading frequencies is required

Δε: DIC and FEA comparison

To determine ΔƐ from the FE model, both max. and min. loading cases were modelled

- For 10 mm debonded specimen case

Maximum load : -1000 N

Minimum load : -100 N

$$\Delta\varepsilon = \varepsilon_{max.load} - \varepsilon_{min.load}$$

- FE corresponds well with DIC
- Clear discrepancy between FE and experimental strains around 2x/L = 0.55,
  - Localised stress concentrations around the loading roller
  - Boundary conditions at the loading roller region were not perfectly modelled
  - Light reflection on the mirror

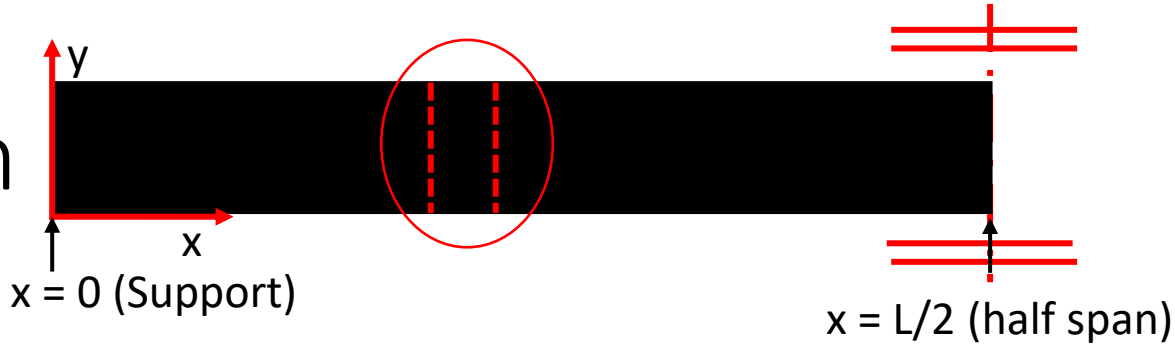

10 mm debonded specimen

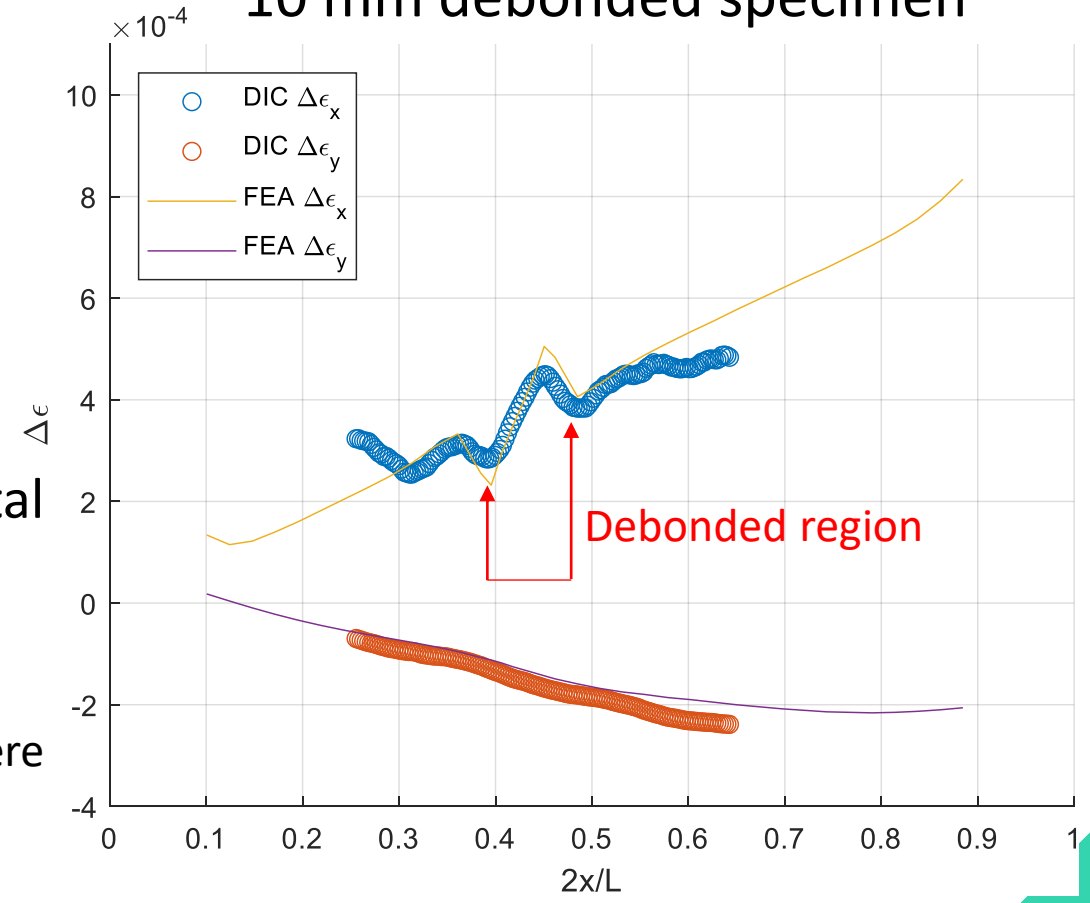

Investigation of face sheet/core interface

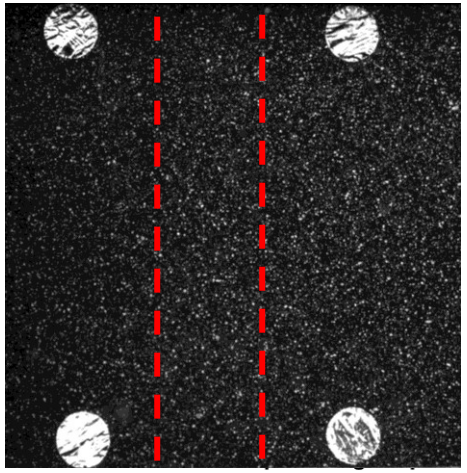

Thermoelastic Stress analysis (TSA)

Obtain thermoelastic response at the damaged region at different frequencies

$$\frac{\Delta T}{T_0} = \frac{(\alpha_1 \Delta\sigma_1 + \alpha_2 \Delta\sigma_2)}{\rho C_p}$$

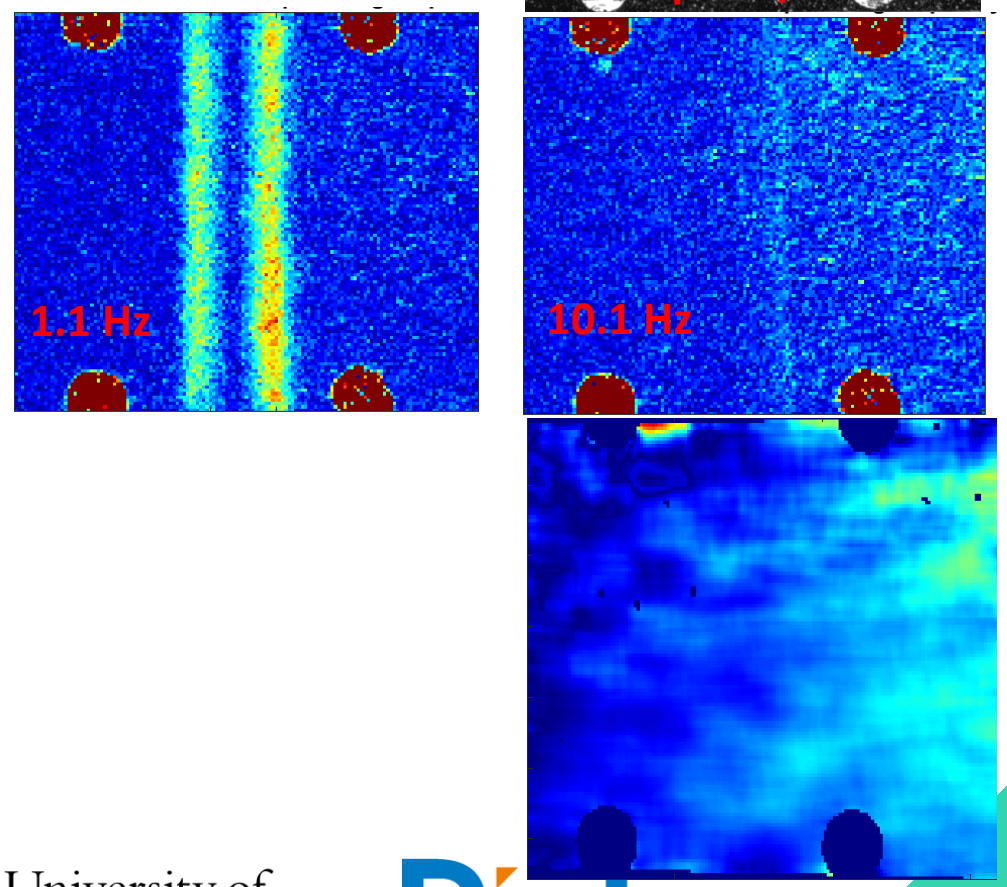

Digital Image correlation (DIC)

Obtain **surface ply** thermoelastic response at 1.1 Hz

$$\frac{\Delta T_{surfaceply}}{T_0} = -\frac{e}{\rho C_p}\begin{bmatrix}\alpha_1 & \alpha_2 & 0\end{bmatrix}\begin{bmatrix}\frac{E_1}{1-\nu_{12}\nu_{21}} & \frac{\nu_{21}E_1}{1-\nu_{12}\nu_{21}} & 0 \\ \frac{\nu_{21}E_1}{1-\nu_{12}\nu_{21}} & \frac{E_2}{1-\nu_{12}\nu_{21}} & 0 \\ 0 & 0 & G_{12}\end{bmatrix}[T_e]\begin{bmatrix}\Delta\varepsilon_x \\ \Delta\varepsilon_y \\ \Delta\varepsilon_{xy}\end{bmatrix}$$

Data Fusion

Thermoelastic response − **Surface thermoelastic response from DIC** =

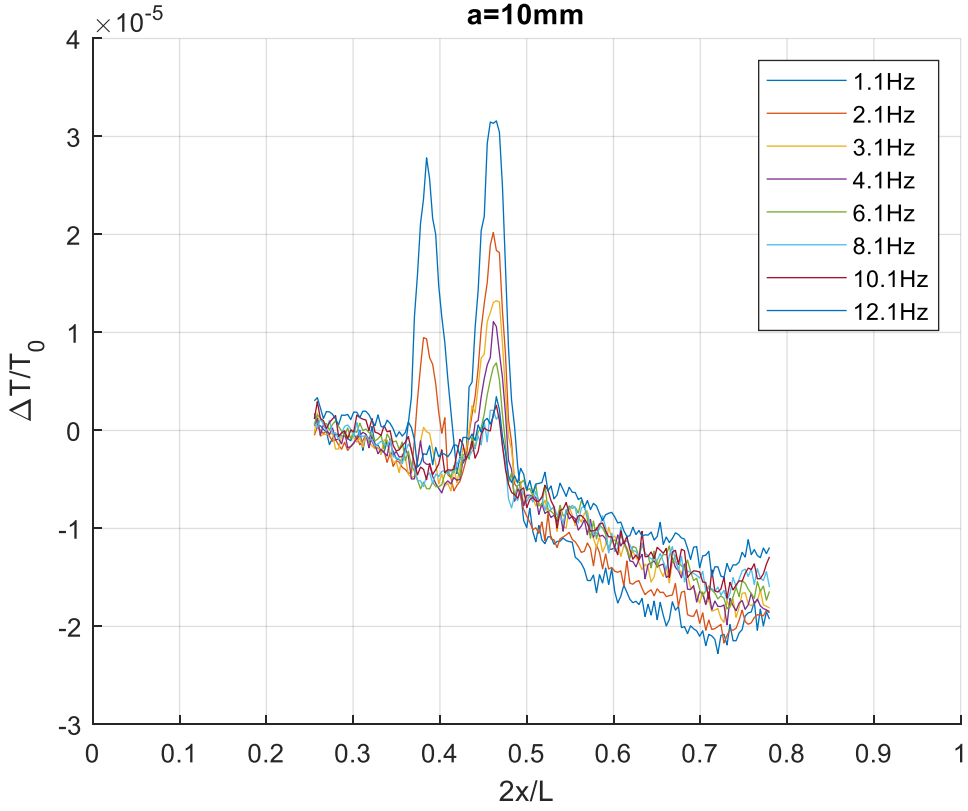

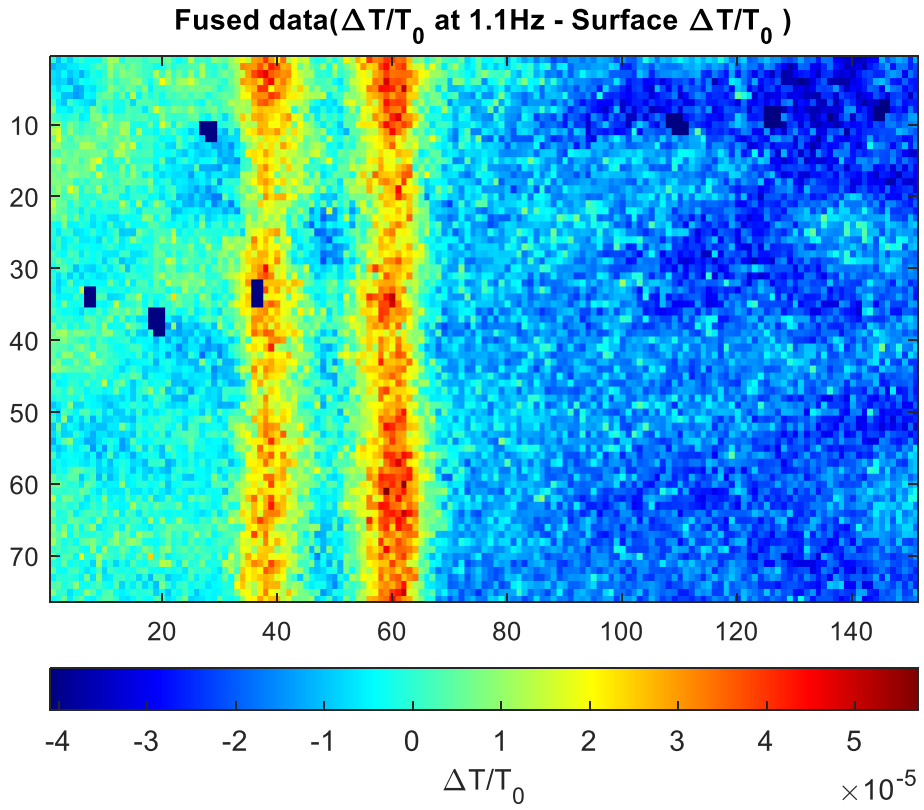

Does this represent the thermoelastic response at the interface ?

Summary and Future work

- Interface debonded was observed through the face sheets using thermoelastic stress analysis, when cyclically loaded at low frequency.

- DIC and FE surface ply strains were closely matched at the debonded region

- A data fusion technique was developed so that the DIC surface ply thermoelastic response could be subtracted from the TSA thermoelastic responses over a range of loading frequency:
  - Thermoelastic model development to understand better the heat transfer effects
  - Identify the source of thermoelastic response in the fused data and relate ΔT to the stress intensity factor at the interface crack tip

- Monitor damage progression and characterize the internal fracture behaviour through the thin face sheets of sandwich structures using DIC, TSA and FE analysis.

UKRI Engineering and Physical Sciences Research Council
CERTIFEST CERTIFICATION FOR DESIGN: RESHAPING THE TESTING PYRAMID
University of BRISTOL
Diab

UKRI Engineering and Physical Sciences Research Council

CERTIFICATION FOR DESIGN: RESHAPING THE TESTING PYRAMID

University of BRISTOL

UNIVERSITY OF BATH

University of Southampton

UNIVERSITY OF EXETER

AIRBUS

BAE SYSTEMS

Rolls-Royce

GKN AEROSPACE

NATIONAL COMPOSITES CENTRE

cfms

The Alan Turing Institute

Thank you for your attention. Any questions?

emily.leung@bristol.ac.uk

Engineering and Physical Sciences Research Council

CERTIFICATION FOR DESIGN: RESHAPING THE TESTING PYRAMID

University of BRISTOL

Diab

DIC processing information

Hardware	Stereo DIC
Cameras	Flir Blackfly S USB3
Sensor and digitization (pixels)	12-bits, 2448 X 2050
Lens	Tokina atx-I 100mm F2.8 FF MACRO PLUS
Imaging distance (m)	~ 1.06
Lighting	Dracast LED500 Pro Series Bi-Color LED Panel Light
Pixel resolution	~ 1 pixel = 0.04 mm

Analysis Parameters	Stereo DIC
DIC software	MatchID
Subset, step size (pixel)	49,20
Interpolation	Local Bicubic Splines
Shape functions	Affine
correlation criterion	ZNSSD
Prefiltering	Gaussian
Strain Window	19
VSG (pixel)	409
Strain Interpolation	Q4
Strain Tensor	Log. Euler-Almansi

DIC processing information

System Performance	
Displacement noise floor (mm)	
u	$\approx 3.50 \times 10^{-4}$
v	$\approx 4.67 \times 10^{-4}$
w	$\approx 2.90 \times 10^{-3}$
strain noise floor (%)	
ε_{xx}	$\approx 8.66 \times 10^{-4}$
ε_{yy}	$\approx 9.69 \times 10^{-4}$
ε_{xy}	$\approx 4.91 \times 10^{-4}$

Reflectivity study of a front coated mirror

- A temperature controlled black body (IR-2106 from Infrared Systems Development Corporation) was used to generate a temperature target.
- A Telops FAST M3k infra-red camera (50 mm lenses) was set-up so that in the first set of the tests the camera viewed the black body through an aluminium front coated mirror (ME8S-G01 from THORLABS) and in the 2nd set of tests the camera viewed the black body directly.
- The temperature of the black body was adjusted and once stable the measurements were taken again.

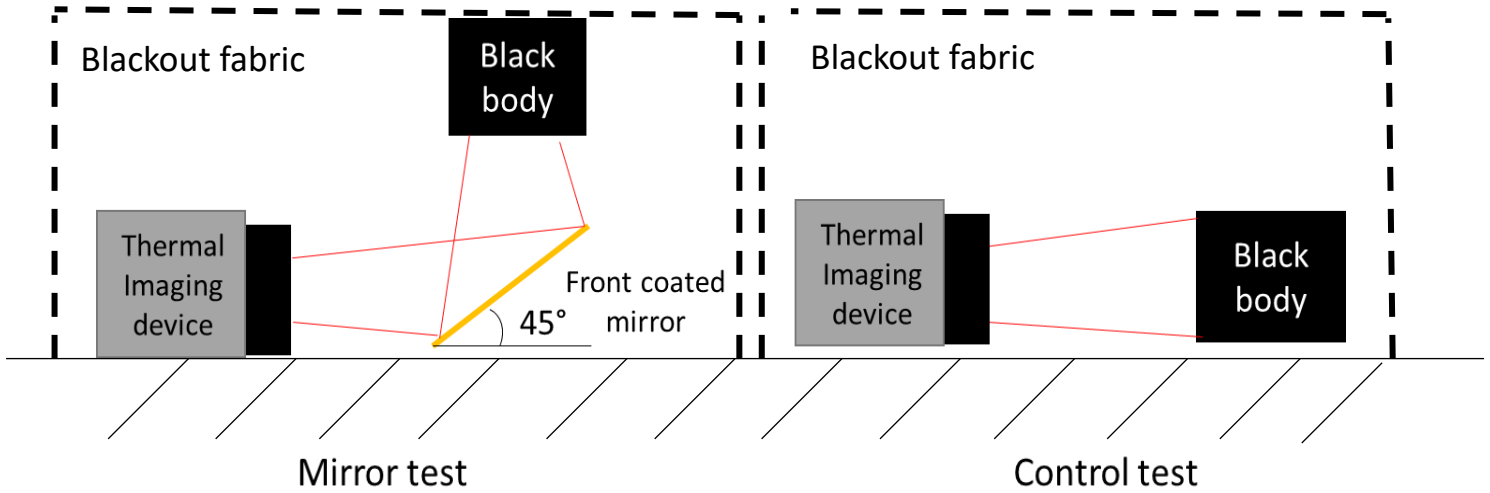

Schematic of mirror testing using thermal imaging device

Reflectivity study of a front coated mirror

The deviation of the slope of the curve from 1 (red line) indicated the attenuation effect of the mirror.

- Small attenuation
- The emissivity of the black body = 0.96 ± 0.02
- The average reflectivity of the mirror is about 0.994 ± 0.004 ≈ 1
- Correction factor is not required

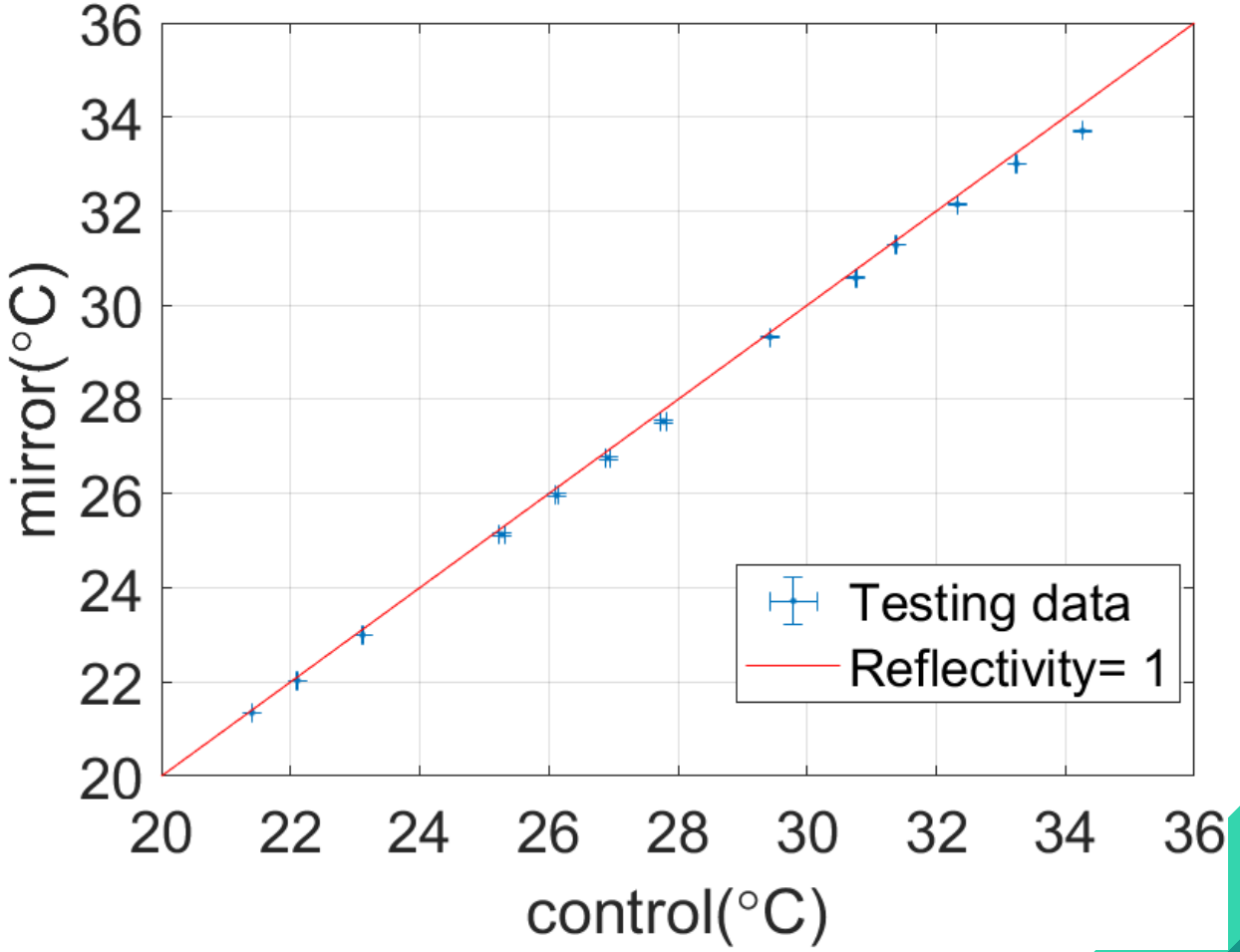

Validate the DIC data captured using mirror

- The DIC displacement : Averaging the field of view.
- The slope of the plot is 0.98 and there is 2 % error.
- Experimental error from the testing machine.
- Error from the noise floor ($w \approx 3.89 \times 10^{-4}$ mm).

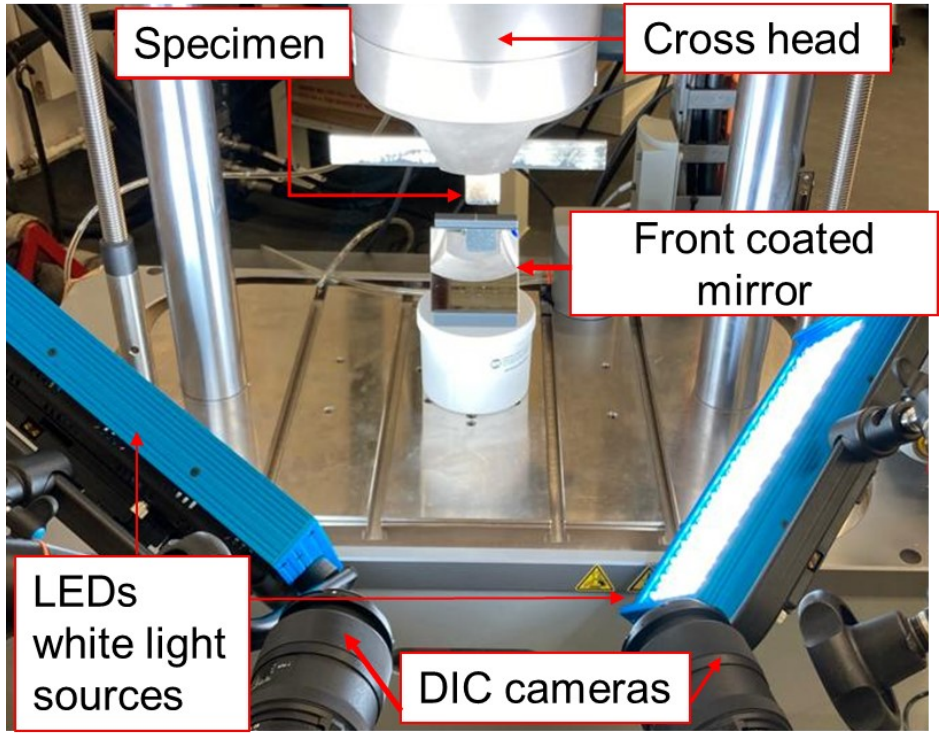

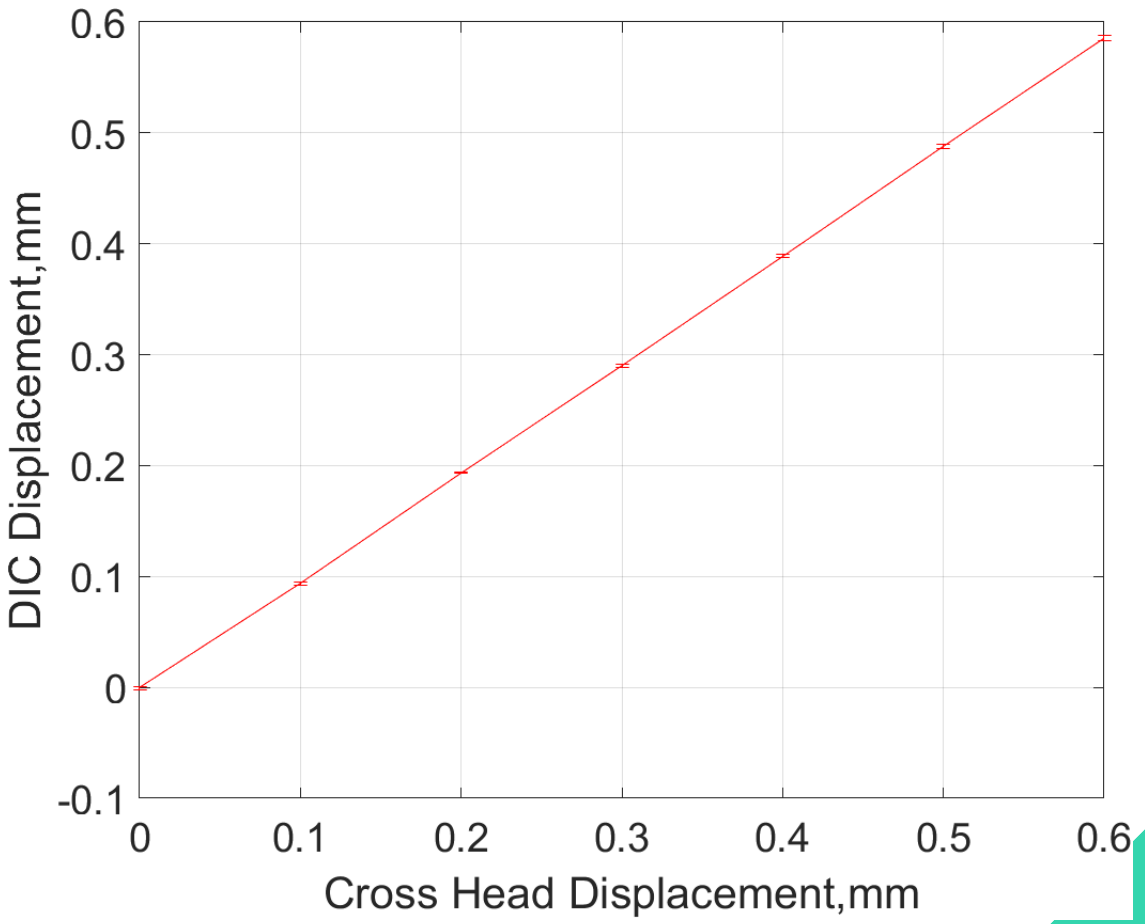

FE modeling details

- A quadrant of the specimen is modeled using the commercial FE package Abaqus/CAE 2018.
- Element types:
  - C3D20-Twenty-node brick element (face sheet and core)
  - Approximate global size at the face sheet and core: 3 mm and 1.5 mm (debonded, supported and indented regions)
  - R3D4- 3D Rigid element (Indenter and support)
  - Approximate global size: 1.5 mm
- Total number of nodes: 124936
- Total number of elements: 27025